

Synthesis of InP nanofibers from tri(m-tolyl)phosphine: an alternative route to metal phosphide nanostructures†

Junli Wang,^{a,b} Qing Yang,^{*a,b} Zude Zhang,^b Tanwei Li^a and Shuyuan Zhang^a

Received 25th June 2009, Accepted 30th September 2009

First published as an Advance Article on the web 3rd November 2009

DOI: 10.1039/b912525f

The synthesis of InP nanofibers *via* a new Ullmann-type reaction of indium nanoparticles with tri(m-tolyl)phosphine (P(PhMe)₃) was typically performed to illustrate an alternative route for the preparation of nanostructured metal phosphides, including III–V (13–15) and transition-metal phosphides. Triarylphosphine compounds such as other two tri(m-tolyl)phosphine isomers, diphenyl(p-tolyl)phosphine, and triphenylphosphine were comparably employed to synthesize InP nanocrystals. From the aspect of the carbonization of triarylphosphines, Raman spectroscopy and thermo-gravimetric analysis (TGA) investigations of the InP products showed that the stability of these triarylphosphines conformed to the order of tri(p-tolyl)phosphine ≈ tri(o-tolyl)phosphine < diphenyl(p-tolyl)phosphine < tri(m-tolyl)phosphine < triphenylphosphine. The correlation between the stability of triarylphosphines and the growth of InP nanocrystals was investigated, and experimental results showed that the relatively stable triarylphosphines (tri(m-tolyl)phosphine and triphenylphosphine) were favorable for the preparation of one-dimensional (1D) InP nanostructures (nanofibers and nanowires). The reactivity (stability) of triarylphosphines was also compared with those of P(SiMe₃)₃ (typically see: J. M. Nedeljković, O. I. Mičić, S. P. Ahrenkiel, A. Miedaner and A. J. Nozik, *J. Am. Chem. Soc.*, 2004, **126**, 2632) and P(C₈H₁₇)₃ (C. Qian, F. Kim, L. Ma, F. Tsui, P. D. Yang and J. Liu, *J. Am. Chem. Soc.*, 2004, **126**, 1195) according to the difference in preparative temperature for phosphide synthesis. Raman and photoluminescence properties of the as-synthesized InP nanocrystals were further studied, and the synthetic mechanism of our method was reasonably investigated by GC-MS analysis. Moreover, the current route was successfully extended to prepare GaP, MnP, CoP and Pd₃P₂ nanocrystals.

Introduction

Group III–V (13–15) compound semiconductors have attracted considerable interest owing to their significant value in fundamental researches and technical applications, including quantum size effects,^{1,2} electronic and optoelectronic devices,^{3–5} which promote researchers to pursue effective methods and chemical reactions for preparing this kind of materials.^{6–21} Among the III–V semiconductors, much attention has been paid to the preparation of GaP, InP and their alloys through various chemical approaches, such as the traditional direct reactions of elements in the solid state at high temperature⁶ or its variation in organic solution phase at relative low temperature,⁷ precursor metathesis reactions in solid state or solution phase,^{8,9} the organometallic routes in both gas-phase and solution phase, including metal organic chemical vapour deposition (MOCVD),^{10,11} metal organic

vapor phase epitaxy (MOVPE)^{12,13} and pyrolysis of single-source organometallic precursors,^{14,15} and dehalosilylation and related reactions.^{16–21}

It is interesting to note that the development of preparative methods for III–V phosphides is, in general, a process which explores suitable phosphorus sources. Elemental red or yellow phosphorus is used in direct elemental reactions to synthesize metal phosphides,^{6,7} and (Na/K)₃P, as a reactive phosphorus source, is often employed in metathesis reactions.^{8,9} Phosphine and trialkylphosphine such as PH₃ and P^tBu₃ are usually used in the organometallic routes to III–V phosphides.^{10–15,22} Recently, an attractive phosphorus source, tris(trimethylsilyl)phosphine (P(SiMe₃)₃), has intensively been present in the controlled synthesis of nanoscale III–V phosphides, and the dehalosilylation and related reactions are proposed.^{16–21} Meanwhile, trioctylphosphine (P(C₈H₁₇)₃, TOP), which is often used as a surfactant or capping agent in the size and shape control of nanocrystals,^{17–19,23} has been employed as a phosphorus precursor to synthesize InP and other metal phosphide nanocrystals.²⁴ At the same time, our group employed triphenylphosphine (PPh₃) as an alternative phosphorus source to prepare InP and GaP nanostructures.²⁵ This successful preparation shows that obtaining elemental phosphorus from organic arylphosphine to synthesize metal phosphides is an effective strategy. Because of the enormous multitude of triarylphosphine compounds, it is believed that triarylphosphine will be a kind of attractive phosphorus source for the preparation of metal phosphides in both bulk and nanoscale forms.

^aHefei National Laboratory for Physical Science at Microscale, University of Science and Technology of China (USTC), Hefei, Anhui 230026, People's Republic of China

^bDepartment of Chemistry, University of Science and Technology of China (USTC), Hefei, Anhui 230026, People's Republic of China. E-mail: qyoung@ustc.edu.cn; Fax: +86-551-3606266; Tel: +86-551-3600243

† Electronic supplementary information (ESI) available: EDX spectrum, ED pattern, HRTEM images and XPS spectra of InP nanofibers, GC-MS data of organic sideproducts, XRD patterns, Raman spectra, and CH analysis of InP samples, XRD patterns of the products after the thermal-treatment of InP samples, TEM images and EDX spectra of the InP, GaP, MnP, CoP and Pd₃P₂ samples. See DOI: 10.1039/b912525f

In this article, we develop the above pathway and use other types of triarylphosphine compounds, such as diphenyl(*p*-tolyl)phosphine and three tritolylphosphine isomers, as phosphorus precursors to prepare metal phosphide nanostructures. The synthesis of one-dimensional (1D) InP nanofibers from the reaction of indium nanoparticles with tri(*m*-tolyl)phosphine (P(PhMe)₃) was typically carried out to illustrate the adaptability and mechanism of our method. The reactivity and carbonization of different triarylphosphine compounds were comparably studied by analyzing the InP products using Raman spectroscopy and thermo-gravimetric analysis (TGA), and the relationship between the reactivity of triarylphosphines and the size and shape of InP products was demonstrated. The Raman and photoluminescence (PL) properties of the as-obtained InP nanocrystals were also investigated. Moreover, the current method was readily extended to synthesize some other metal phosphides such as GaP, MnP, CoP and Pd₃P₂ nanocrystals.

Experimental section

Synthesis of InP nanofibers

All materials were used as received without further purification. In a typical synthesis of InP nanofibers, a mixture of 0.114 g (1 mmol) newly-prepared indium nanoparticles^{26a} and 0.330 g (1.1 mmol) tri(*m*-tolyl)phosphine was added into a quartz ampoule (ϕ 1 cm \times 15 cm), which was then evacuated and sealed. The sealed ampoule was horizontally loaded in a resistance furnace at 370 \pm 2 $^{\circ}$ C for 8–15 h. The temperature was increased from room temperature to the reaction temperature over 100 min. After the ampoule was naturally cooled to room temperature, the black products were collected, washed with benzene, diluted hydrochloric acid and absolute alcohol, and finally dried under vacuum at 60 $^{\circ}$ C for further investigation. Similarly, InP nanocrystals can be prepared by replacing tri(*m*-tolyl)phosphine with tri(*p*-tolyl)phosphine, tri(*o*-tolyl)phosphine or diphenyl(*p*-tolyl)phosphine. The synthetic details are in summarized Table 1.

Synthesis of GaP, MnP, CoP and Pd₃P₂ nanocrystals

The synthesis procedures for GaP, MnP, CoP and Pd₃P₂ nanocrystals were analogous to those that were used to synthesize InP nanofibers from tri(*m*-tolyl)phosphine except the change of corresponding metals. Ga, Mn and Co powdered metals were

Table 1 Summary of the synthesis of various metal phosphide nanocrystals at different experimental conditions^a

Metals	Triarylphosphines	<i>T</i> / $^{\circ}$ C	Products
In	tri(<i>m</i> -tolyl)phosphine	370	InP nanofibers
In	tri(<i>m</i> -tolyl)phosphine	390	InP NPs + amorphous C
In	tri(<i>o</i> -tolyl)phosphine	370	InP NPs + amorphous C
In	tri(<i>p</i> -tolyl)phosphine	370	InP NPs + amorphous C
In	diphenyl(<i>p</i> -tolyl)phosphine	370	InP NPs + amorphous C
In	triphenylphosphine	370–390	InP nanowires ²⁵
Ga	tri(<i>m</i> -tolyl)phosphine	370	GaP NPs
Mn	tri(<i>m</i> -tolyl)phosphine	370	MnP NPs
Co	tri(<i>m</i> -tolyl)phosphine	370	CoP NPs
Pd	tri(<i>m</i> -tolyl)phosphine	370	Pd ₃ P ₂ NPs

^a NPs denoted nanoparticles in the table

purchased from Alfa Aesar and used as received, while Pd particles were obtained by a polyol-reduced synthesis.^{26b} All of the syntheses were carried out for 12 h with the metal/tri(*m*-tolyl)phosphine molar ratio of 1 : 1.1. The preparation conditions for the GaP, MnP, CoP and Pd₃P₂ nanocrystals are shown in Table 1.

Characterization

The as-prepared products were characterized by powder X-ray diffraction (XRD) using a Philips X' Pert Pro Super diffractometer with graphite-monochromatized Cu K α radiation (λ = 1.54178 \AA). Morphologies and microstructures of the samples were examined by scanning electron microscopy (SEM, JEOL JSM-6700F), transmission electron microscopy (TEM, JEOL-2010), selected area electron diffraction (SAED), and high-resolution TEM (HRTEM, JEOL-2010, used with an accelerating voltage of 200 kV). Energy-dispersive X-ray spectroscopy (EDX) was recorded on an Oxford ISIS spectroscope attached to HRTEM. X-Ray photoelectron spectroscopy (XPS) was performed with an ESCALab MKII X-ray photoelectron spectrometer, using Al K α X-rays as the excitation source. The binding energies obtained in the XPS analysis were calibrated against the C 1s peak at 284.6 eV. The gas chromatography-mass spectrometry (GC-MS) of benzene solution of organic byproducts produced in the synthesis was performed with a Micromass GCT TOF mass spectrometer. Raman and photoluminescence (PL) spectra of the InP sample were recorded on a Jobin Yvon HR800 (Horiba group) spectrometer using the 514.5 nm line of an Ar⁺ ion laser for excitation. Thermogravimetric analysis (TGA) was performed using a DTG-60H instrument (Shimadzu Company) at a heating rate of 10 $^{\circ}$ C min⁻¹. The CH analysis of InP samples was carried out on Elementar Vario EL III (German) with the temperature up to 950 $^{\circ}$ C.

Results and discussion

As outlined in Table 1, some nanostructured metal phosphides have been prepared from the reactions of elemental metals with triarylphosphine compounds by our method. The synthesis of InP nanofibers from In nanoparticles and tri(*m*-tolyl)phosphine is typically used to demonstrate the synthetic mechanism and the generality of the current route. Fig. 1 shows a SEM image of InP nanofibers, revealing the InP products are composed of almost 1D fiber-like nanostructures that have diameters of 50 to 200 nm and lengths of up to several hundreds of nanometers. The elemental composition of InP nanofibers has been characterized by EDX spectroscopy, and the results (Fig. S1 in the ESI†) confirm

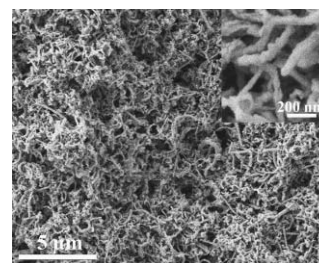


Fig. 1 SEM image of InP nanofibers synthesized from In/tri(*m*-tolyl)phosphine at 370 $^{\circ}$ C for 12 h.

that the molar ratio of In:P is about 1:1. The XRD pattern of InP nanofibers is shown in Fig. 2, which shows the good crystallizability of the products. Further analyses of the peaks in the XRD pattern indicate that zinc-blend (ZB) structured InP (JCPDS No. 73-1983) is dominant in the nanofibers, and that the two weak peaks near the (111) peak of ZB InP can be readily indexed to the (100) and (101) planes from wurtzite (W) InP.

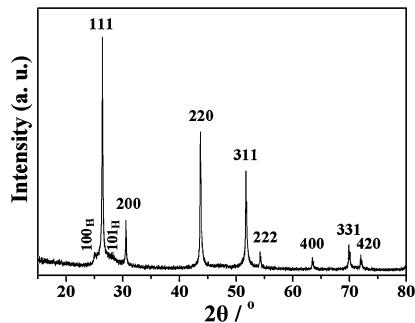


Fig. 2 XRD pattern of InP nanofibers synthesized from In/tri(m-tolyl)phosphine at 370 °C for 12 h.

The morphology and microstructural details of InP nanofibers are further provided by means of TEM, ED and HRTEM techniques. Fig. 3a and b are TEM images of InP nanofibers, which is in agreement with the SEM observation. Interestingly, the curved spring-like InP nanostructures can be produced in the synthesis (Fig. 3b). These novel spring-like or ring-like nanostructures were only reported by several groups *via* a thermal deposition process.²⁷ Fig. 3c shows the HRTEM image and ED pattern of ZB InP nanofibers, revealing the good crystallizability and the [111] growth direction of ZB InP nanowires. Shown in Fig. 3d are the HRTEM image and the corresponding ED pattern recorded on W InP nanofibers, which can be well indexed to the [210] zone axis of W InP, and it can be observed that the W InP nanofibers grow

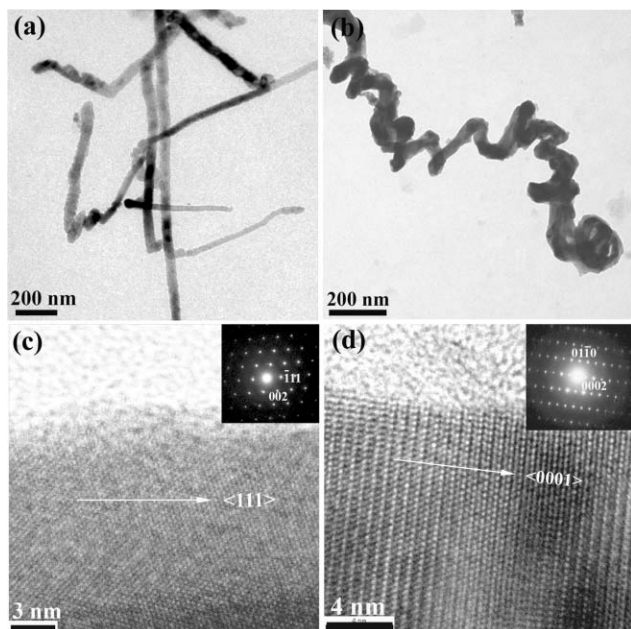
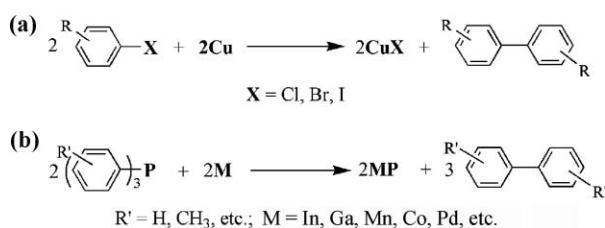


Fig. 3 TEM images of the InP nanofibers (a, b); HRTEM image and ED pattern recorded on ZB InP nanofibers (c) and W InP nanofibers (d).

in the [001] direction. Meanwhile, stacking faults and twinning structures were further observed in the InP nanofibers by HRTEM and ED investigations (Fig. S2[†]), from which it is interesting to note that twins are present vertical to the growth direction of InP nanofiber, which is different from the common cases where twinning structures often occur in 1D ZB InP or other semiconductor nanostructures along their growth direction (the $\langle 111 \rangle$ directions).²⁸ The HRTEM and ED investigations also show that the growth direction of the InP nanofiber is the $\langle 211 \rangle$ direction and the intergrowth of W and ZB structures is present in the InP nanofiber (Fig. S2[†]).

Furthermore, XPS spectra were taken to examine the quality and surface composition of InP nanofibers (Fig. S3[†]), which indicates the presence of In and P along with C from the reference and O from absorbed species. In the high-resolution XPS spectra of the In 3d region, the peak of In 3d_{5/2} is centered at 444.62 eV (Fig. S3b[†]), which can be attributed to indium from InP.⁷ In the close-up P 2p spectrum for the P core, there are two peaks (Fig. S3c[†]). The peak at 128.61 eV, agreeing with P from InP, is much stronger than the other one at 133.6 eV, assigned to P from oxidized P species,⁷ demonstrating the high purity of the as-synthesized InP products.

In the present work, tri(m-tolyl)phosphine was typically used as a phosphorus source for the synthesis of InP nanofibers. In this process, the phosphorus element was extracted from tri(m-tolyl)phosphine and combined with liquid indium droplets to produce InP nanocrystals. From the aspect of the valence change, metallic indium was oxidized by tri(m-tolyl)phosphine to In(III) of InP nanocrystals, whereas tri(m-tolyl)phosphine served as both an oxidant and phosphorus precursor and then transferred to organic byproducts after the extraction of phosphorus in the synthesis. The simplicity of our synthetic system such as the use of a sealed vacuum ampoule and no addition of surfactants is favorable for studying the reaction mechanism for the current synthesis. In order to clarify the reaction mechanism, the GC-MS technique was employed to analyze the components of organic byproducts produced in the synthesis. The GC-MS measure (Fig. S4[†]) shows the obvious presence of 3,3'-dimethylbiphenyl ($m/z = 182.11$) and other biaryls such as biphenyl ($m/z = 154.08$) and methylbiphenyl ($m/z = 168.10$), indicating that In-P and C-C bonds formed with the cleavage of P-C bonds of tri(m-tolyl)phosphine. The production of biaryls are derived from the coupling of tolyl from tri(m-tolyl)phosphine, and biphenyl and methylbiphenyl are probably produced with the breaking off methyl from dimethylbiphenyl due to the lower stability of tolyl in comparison with phenyl at elevated reaction temperature (370 °C). With comparison to our previous studies²⁵ and the traditional Ullmann reaction that is one type of copper-catalyzed coupling reactions between aryl halides for the synthesis of biaryls (Scheme 1),²⁹ the reaction mechanism for the current synthesis can be nominated as a new Ullmann-like reaction in the view of the coupling of aryls catalyzed by metals (Scheme 1). The reaction mechanism can be supported by some previous work reported by several groups, for example, In(0) droplets reacted with P(SiMe₃)₃ to prepare InP nanocrystals *via* the cleavage of P-Si bonds of P(SiMe₃)₃,¹⁸ and InP and FeP nanocrystals could be synthesized *via* catalytic cleavage of P-C bonds of TOP to *in situ* generate phosphorus atoms that reacts with In and Fe particles to form InP and FeP, respectively.²⁴ However, the detailed reaction mechanism



Scheme 1 (a) The traditional Cu-catalyzed Ullmann reaction, and (b) the new Ullmann-like reaction for metal phosphide syntheses, by which biaryls and inorganic compounds (CuX and MP) are produced.

was not studied from the view of examining the components of organic byproducts, owing to the instabilities of alkyl groups from TOP and the complexities of the preparative systems with the addition of surfactants. Our work showed that the new Ullmann-like reaction can provide an alternative and general chemical route to prepare metal phosphides in the bulk or nanoscale form.

For the above-mentioned three kinds of phosphorus sources, the bond stabilities of P–Si bonds and P–C bonds affect the extraction of phosphorus element. Generally, the higher bond energy makes the bond more difficult to break, and thus the extraction of phosphorus is more difficult, which can be reflected by the difference in the preparative temperature employed. On the basis of the reported literature, it is noted that the temperature when using $\text{P}(\text{SiMe}_3)_3$ (220–320 °C)^{16–21} as phosphorus source is generally lower than that using TOP (300–370 °C)²⁴ in the synthesis of metal phosphide nanocrystals. Moreover, InP and other metal phosphide nanocrystals can be often prepared from reactions between metal precursors and $\text{P}(\text{SiMe}_3)_3$ in the TOP medium.^{17–19} This case also shows that the extraction of phosphorus from $\text{P}(\text{SiMe}_3)_3$ is easier than that from TOP. In our synthesis of InP nanocrystals using triarylphosphine including tri(m-tolyl)phosphine and triphenylphosphine, the suitable reaction temperature is around 360–400 °C,²⁵ which is a little higher than those employed for the syntheses of metal phosphide nanocrystals using TOP phosphorus source. This result reveals that the cleavage of P–C bond from triarylphosphine is more difficult than that of P–C bond from TOP, that is to say, P–C bond from triarylphosphine is more stable than P–C bond from TOP. Therefore, it can be concluded that the difficult trend in the extraction of phosphorus element from the three phosphorus sources is in the order of $\text{P}(\text{SiMe}_3)_3 < \text{TOP} < \text{triarylphosphine}$ (PPh_3 and $\text{P}(\text{PhMe}_2)_3$).

In the Raman spectrum of InP nanofibers (Fig. 4a), the peaks at around 301 and 339 cm^{-1} correspond to the transverse optical (TO) and longitudinal optical (LO) phonon modes of InP, respectively. The resonance frequencies of TO and LO modes from InP nanofibers are slightly red-shifted from those of bulk InP (TO = 308 cm^{-1} , LO = 348 cm^{-1}),³⁰ which may be caused by the effects of small size and high surface area of the sample.³¹ The two weak peaks at 606 and 674 cm^{-1} are indexed to the second TO and LO modes of InP. Based on the relative intensity of Raman peaks from InP nanofibers and from amorphous carbon (1362 and 1692 cm^{-1}),³² one can see that there is only a very small quantity of carbon in the InP nanofibers prepared from In/tri(m-tolyl)phosphine at 370 °C for 12 h, and that the nanofibers are of high purity.

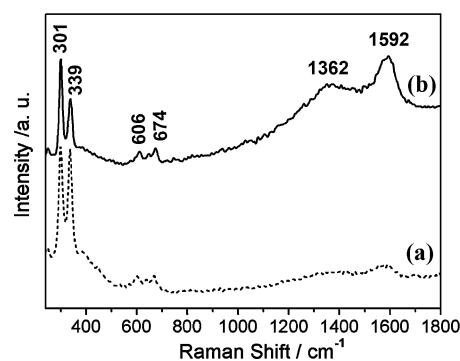


Fig. 4 Raman spectra for (a) the InP nanofibers prepared from In/tri(m-tolyl)phosphine at 370 °C for 12 h, and (b) the InP products prepared from In/tri(m-tolyl)phosphine 390 °C for 12 h.

As shown in Fig. 4, the variations in relative intensity of Raman peaks from amorphous C reveal that the degree of the carbonization of tolyl from tri(m-tolyl)phosphine at 390 °C is obviously greater than that at 370 °C. As for PPh_3 , however, the carbonization of phenyl is not obviously observed even at 390 °C.²⁵ The results show that tri(m-tolyl)phosphine is easier to be carbonized than PPh_3 . On the basis of Raman analyses (Fig. S5†), it is also found that the carbonization of tri(p-tolyl)phosphine, tri(o-tolyl)phosphine and diphenyl(p-tolyl)phosphine is easier than that of tri(m-tolyl)phosphine at the same temperature. From the aspect of the carbonization degree of aryls, the stability of triarylphosphines can be concluded as follows: tri(p-tolyl)phosphine \approx tri(o-tolyl)phosphine < diphenyl(p-tolyl)phosphine < tri(m-tolyl)phosphine < triphenylphosphine. The stability order agrees with the principles in organic chemistry. Because the phosphorus atom of triarylphosphine can be considered as an electron donor and thus has activation to methyl in tolyl, tritolylphosphine or diphenyl(p-tolyl)phosphine is more reactive than to triphenylphosphine. Furthermore, the activation of phosphorus atom to p- or o-methyl is greater than that to m-methyl. The activation discipline is readily consistent with aryl halides in the traditional Ullmann reaction.²⁹ The activation causes the poor thermal stability, which will lead to the carbonization of triarylphosphine. The above stability order can be utilized for designing suitable experiments to control the growth of metal phosphide nanocrystals with special size and shape. For instance, the reactions of indium nanoparticles with reactive tri(p-tolyl)phosphine, tri(o-tolyl)phosphine or diphenyl(p-tolyl)phosphine produce InP nanocrystals with an irregular spherical shape (Fig. S6†), whereas InP nanofibers can be synthesized from stable tri(m-tolyl)phosphine or triphenylphosphine.

Thermo-gravimetric analysis (TGA) was further used to measure the content of amorphous C and the thermal stability of InP nanofibers in air, and some interesting results were found. Fig. 5 shows the TGA curves that were collected at a heating rate of 10 °C min^{-1} . TGA results show that the distinct changes of the as-synthesized InP products occurred in the heat treatment in air (O_2) from room temperature to 800 °C. Fig. 5a is the TGA curve for the InP nanofibers prepared from In/tri(m-tolyl)phosphine at 370 °C, while Fig. 5b shows the one for the InP products prepared from In/tri(m-tolyl)phosphine at 390 °C. The final products after heat-treated were examined with XRD, and the XRD patterns (Fig. S7†) show that the final products are InPO_4 , In_2O_3 and

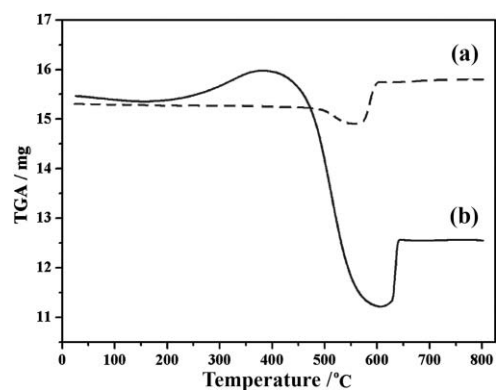


Fig. 5 TGA results for (a) the InP nanofibers prepared from In/tri(m-tolyl)phosphine at 370 °C for 12 h, and (b) the InP products prepared from In/tri(m-tolyl)phosphine at 390 °C for 12 h.

$\text{In}(\text{PO}_3)_3$. These results are consistent with the cases reported in previous literature.³³ The analyses of TGA and XRD show that some obvious changes and chemical reactions of InP nanocrystals take place in the heat treatment in O_2 . In the TGA analysis for InP nanofibers, the first weight loss lies in the temperature range 25–200 °C, which is attributed to the elimination of surface capping groups such as some volatile or decomposable organic components and adsorbed water in the starting InP nanofibers. As the temperature rises, a pronounced weight loss step is found in the TGA curve in the temperature range of 340–565 °C in air (O_2), which can be ascribed to the loss of phosphorus of InP nanofibers ($\text{InP} \rightarrow \text{InO}_{3/2}$) and the burnoff of carbon. In this step the weight-loss value is 7.16% given by TGA, and in comparison with that of 4.8% from InP to $\text{InO}_{3/2}$ theoretically. Meanwhile, the volatilization of the sample is probably occurred along with the above reaction. Obviously, the maximal carbon content in the InP nanofibers is no more than 2.4%, which shows the high purity of InP nanofibers. There is a distinct weight-gain step in the temperature range of 565–610 °C in the TGA curve, which is attributed to the chemical change from InP to InPO_4 . The TGA curve (Fig. 5b) for InP products prepared at 390 °C has a similar character to that for InP nanofibers with some difference of temperature range. In this curve, there is an obvious weight loss process in the temperature of 385–605 °C, and the weight-loss value is 30.78%. This weight loss process ascribed to the burnoff of carbon and the loss of phosphorus, and the large weight loss reveals the existence of a considerable quantity of amorphous carbon in the InP products prepared at 390 °C, which agrees well with the Raman measure. At the same time, the CH element analysis was further employed to detect the amorphous carbon content, which shows that the C content in the InP nanofibers is about 1.49%, while a high C content is present in the InP sample synthesized at 390 °C (Fig. S8†). Both the CH and TGA studies show that high temperature results in a large quantity of amorphous C in the InP products.

We further investigated the room-temperature PL property of InP nanofibers prepared from the reaction of In/tri(m-tolyl)phosphine at 370 °C for 12 h. The nanofibers display a red-shifted emission spectrum (Fig. 6a), and the emission peak is centered at 960 nm (For bulk InP, $E_g = 1.35$ eV, 920 nm, at room temperature). The red-shifted emission in the PL spectrum for InP nanofibers can be attributed to impurity-related emission

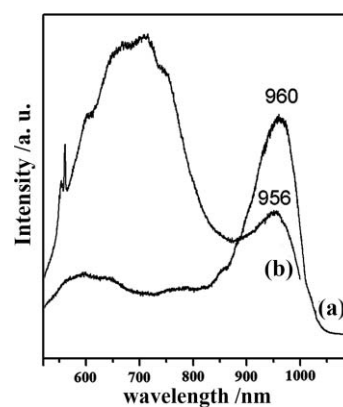


Fig. 6 Room-temperature photoluminescence (PL) spectra of (a) the InP nanofibers prepared from In/tri(m-tolyl)phosphine at 370 °C for 12 h, and (b) the InP products prepared from In/tri(m-tolyl)phosphine at 390 °C for 12 h.

in InP.³⁴ The PL spectrum was also performed for the InP products prepared at 390 °C (Fig. 6b). In the spectrum, the peak at 956 nm is attributed to impurity-related emission in InP, which is similar to the PL emission of InP nanofibers. The broad peak ranging from 520 nm to 870 nm may be from the emission of amorphous C in the InP products prepared at 390 °C,³⁵ and the sharp peak at 565 nm is consistent with the Raman resonance of amorphous C.

In the synthesis, the starting materials are air-stable, low toxic and in solid state, which greatly simplifies the preparative procedures and is friendly to operators. When heated to the temperature (370 °C) above the melting points of starting materials, tri(m-tolyl)phosphine becomes liquid and serves as both reaction medium and phosphorus source for the preparation of InP nanofibers. The reaction in a liquid medium will improve the mass transfer and incorporation rate of indium and phosphorus atoms, and thus InP nanofibers can be conveniently produced *via* the current developed Ullmann-type reaction (Scheme 1). Meanwhile, liquid triarylphosphine itself can act as a surfactant stabilizer and capping reagent to confine the InP nanofiber growth, because tri(m-tolyl)phosphine with a nonbonding lone pair of electrons of the phosphorus atom can be used as a nucleophile to attract metal atoms,²⁵ which is analogous to TOP.^{17–19,24} The present method for InP nanofibers is carried out without the need for highly toxic and reactive phosphorus precursors, the lone time and high temperature, which is more facile and desirable for preparation of metal phosphide nanocrystals.

The growth mechanism of InP nanofibers was attributed to an In-catalyzed solution-liquid-solid (SLS) model.^{7,18,19b,21,22} In the InP nanofiber growth at 370 °C, indium nanoparticles (the melting point for bulk In: 154 °C) become liquid droplets and serve as a catalyst to direct InP growth in a preferred orientation. It is noted that the SLS growth mechanism normally has two typical characters: the small liquid droplet catalyst and the curved wire-like products.^{7,18,19b,21,22} The SLS growth model is available for the growth of InP nanofibers in the current route, since the as-obtained InP products (Fig. 1 and 2a,b) are consistent with the above two characters. Meanwhile, the steric effects of tri(m-tolyl)phosphine also induced the formation of 1D InP nanofibers. Tri(m-tolyl)phosphine with a nonbonding lone pair of electrons in phosphorus atom has a similar steric conformation to PPh_3 ,

TOP and TOA,^{15,23,25} and can serve as a surfactant stabilizer and capping reagent to kinetically direct the preferred growth of InP nanofibers. Moreover, the steric effects can usually produce metastable structures,^{15,25b} and therefore it is considered that the high steric effects of tri(m-tolyl)phosphine is a significant factor to induce the formation of metastable W InP nanofibers.

Inspired by the successful synthesis of InP nanofibers, we have extended the present method to other types of metal phosphide nanocrystals. GaP, MnP, CoP and Pd₅P₂ nanocrystals were synthesized from the reaction of corresponding metals with tri(m-tolyl)phosphine at 370 °C for 12 h (Table 1). The phase purity and the crystal structure of these phosphide nanocrystals have been verified by examining their XRD patterns (shown in Fig. 7). All of the diffraction peaks can be indexed to pure cubic GaP (JCPDS No. 32-0397), orthorhombic MnP (JCPDS No. 89-4841), orthorhombic CoP (JCPDS No. 89-4862), and Pd₅P₂ (JCPDS No. 19-0887), respectively. No other peaks from impurities were detected. The SEM (Fig. 8) and TEM studies (Fig. S9†) show the GaP, MnP, CoP and Pd₅P₂ products are irregular spherical nanoparticles. The EDS spectra (Fig. S10†) further confirm the chemical compositions of the phosphide products. The difference in morphologies of these nanoscale metal phosphides and InP nanofibers is probably attributed to different catalysis of metals and intrinsic crystal structures of phosphides.^{24d,25b} The above results show that the new Ullmann-type reaction between metals and triarylphosphines is effective and general for synthesizing nanoscale metal phosphides.

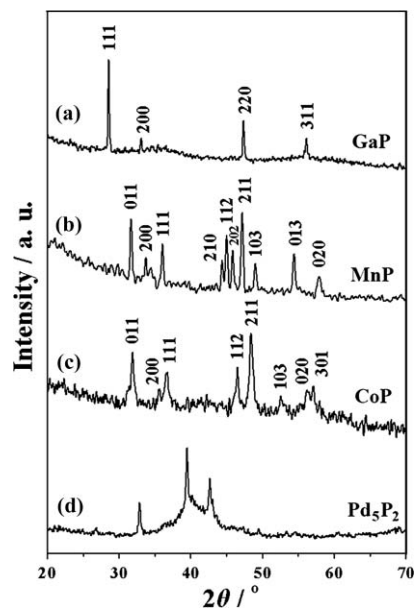


Fig. 7 XRD patterns of the samples: (a) GaP, (b) MnP, (c) CoP, and (d) Pd₅P₂. The diffraction peaks of the XRD pattern for Pd₅P₂ are not assigned since the structure of Pd₅P₂ has not been revealed to date (JCPDS No. 19-0887).

Conclusions

In summary, we synthesized high-quality InP nanofibers from new Ullmann-type reaction of indium nanoparticles with tri(m-tolyl)phosphine. Triarylphosphines such as other two isomers of tri(m-tolyl)phosphine, diphenyl(p-tolyl)phosphine and triph-

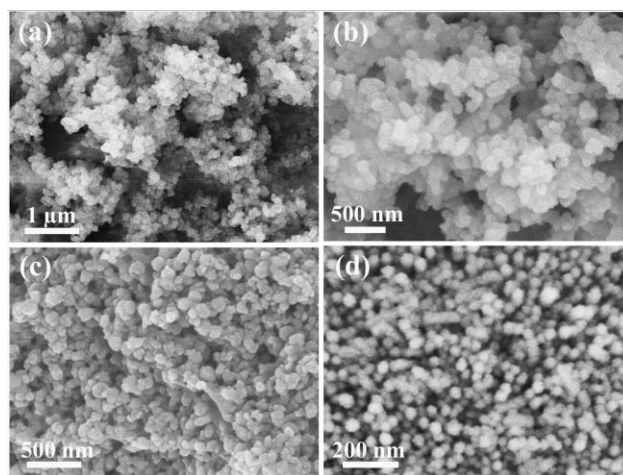


Fig. 8 SEM images of the samples: (a) GaP, (b) MnP, (c) CoP, and (d) Pd₅P₂.

enylphosphine were also comparably studied in the synthesis. On the basis of the carbonization degree of aryls, Raman and TGA analyses showed that the stability of these triarylphosphines adhered to the order: tri(p-tolyl)phosphine \approx tri(o-tolyl)phosphine < diphenyl(p-tolyl)phosphine < tri(m-tolyl)phosphine < triphenylphosphine, and the stable triarylphosphines were favorable for the preparation of InP nanofibers and nanowires, whereas more reactive ones tended to produce irregular InP nanoparticles. The reactivity of P(SiMe₃)₃, TOP, PPh₃ and tri(m-tolyl)phosphine was also compared in the order: P(SiMe₃)₃ < TOP < tri(m-tolyl)phosphine < PPh₃ according to the difference in preparative temperature employed in metal phosphide syntheses. The above rules could be utilized to design suitable experiments and control the growth of metal phosphide nanocrystals with special size and shape. Moreover, the new Ullmann-type reaction route to InP nanofibers was extended to prepare other types of metal phosphide nanocrystals, including GaP, MnP, CoP and Pd₅P₂, which showed the generality of our method. We are convinced that this route will be an attractive strategy for the preparation of metal phosphides.

Acknowledgements

We gratefully acknowledge the financial support from the National Nature Science Foundation of China (Grants 20571068, 20621061), the Program for New Century Excellent Talents at the university from Chinese Ministry of Education (NCET2006-0552), the Anhui Provincial Education Department (KJ2008A071), the Creative Research Foundation for Graduate of USTC (No. KD2008019), and the CAS Special Grant for Post-graduate Research, Innovation and Practice (2008). Meanwhile, Q. Yang acknowledges the project supported by the K. C. Wong Education Foundation of Hong Kong, and thanks Professor Shouheng Sun at Brown University for his kind host for the project.

Notes and references

- L. E. Brus, *J. Chem. Phys.*, 1983, **79**, 5566.
- F. Wang, H. Yu, J. Li, Q. Hang, D. Zemlyanov, P. C. Gibbons, L. W. Wang, D. B. Janes and W. E. Buhro, *J. Am. Chem. Soc.*, 2007, **129**, 14327.

- 3 (a) S. Nakamura, *Science*, 1998, **281**, 956; (b) U. C. Johnson, H. J. Choi, K. P. Knutsen, R. D. Schaller, P. D. Yang and R. J. Saykally, *Nat. Mater.*, 2002, **1**, 106.
- 4 X. Jiang, Q. Xiong, S. Nam, F. Qian, Y. Li and C. M. Lieber, *Nano Lett.*, 2007, **7**, 3214.
- 5 (a) C. Thelander, P. Agarwal, S. Brongersma, J. Eymery, L. F. Feiner, A. Forchel, M. Scheffler, W. Riess, B. J. Ohlsson, U. Gösele and L. Samuelson, *Mater. Today*, 2006, **9**, 28; (b) C. J. Novotny, E. T. Yu and P. K. L. Yu, *Nano Lett.*, 2008, **8**, 775.
- 6 (a) N. N. Greenwood and A. E. Earnshaw, *Chemistry of the Elements*, Pergamon Press, New York, 1994; (b) P. Hagemuller, *Preparative Methods in Solid State Chemistry*, Academic Press, New York, 1972.
- 7 P. Yan, Yi. Xie, W. Z. Wang, F. Y. Liu and Y. T. Qian, *J. Mater. Chem.*, 1999, **9**, 1831.
- 8 (a) R. E. Treece, G. S. Macala, L. Rao, D. Franke, H. Eckert and R. B. Kaner, *Inorg. Chem.*, 1993, **32**, 2745; (b) I. P. Parkin, *Chem. Soc. Rev.*, 1996, **25**, 199.
- 9 S. S. Kher and R. L. Wells, *Chem. Mater.*, 1994, **6**, 2056.
- 10 C. J. Novotny and P. K. L. Yu, *Appl. Phys. Lett.*, 2005, **87**, 203111.
- 11 I. T. Im, H. J. Oh, M. Sugiyama, Y. Nakano and Y. Shimogaki, *J. Cryst. Growth*, 2004, **261**, 214.
- 12 X. G. Xu, Ch. Giesen, R. Hovel, M. Heuken and K. Heime, *J. Cryst. Growth*, 1998, **191**, 341.
- 13 (a) J. Johansson, L. S. Karlsson, C. P. T. Svensson, T. Martensson, B. A. Wacaser, K. Deppert, L. Samuelson and W. Seifert, *Nat. Mater.*, 2006, **5**, 574; (b) M. A. Verheijen, G. Immink, T. de Smet, M. T. Borgström and Erik P. A. M. Bakkers, *J. Am. Chem. Soc.*, 2006, **128**, 1353.
- 14 M. Green and P. O'Brien, *Chem. Commun.*, 1998, 2459.
- 15 Y. H. Kim, Y. W. Jun, B. H. Jun, S. M. Lee and J. Cheon, *J. Am. Chem. Soc.*, 2002, **124**, 13656.
- 16 (a) S. M. Stuczynski, R. L. Opila, P. Marsh, J. G. Brennan and M. L. Steigerwald, *Chem. Mater.*, 1991, **3**, 379; (b) S. R. Aubuchon, A. T. McPhail, R. L. Wells, J. A. Giambra and J. R. Bowser, *Chem. Mater.*, 1994, **6**, 82; (c) R. L. Wells and W. L. Gladfelter, *J. Cluster Sci.*, 1997, **8**, 217.
- 17 S. P. Ahrenkiel, O. I. Mičić, A. Miedaner, C. J. Curtis, J. M. Nedeljković and A. J. Nozik, *Nano Lett.*, 2003, **3**, 833.
- 18 J. M. Nedeljković, O. I. Mičić, S. P. Ahrenkiel, A. Miedaner and A. J. Nozik, *J. Am. Chem. Soc.*, 2004, **126**, 2632.
- 19 (a) D. Battaglia and X. G. Peng, *Nano Lett.*, 2002, **2**, 1027; (b) D. D. Fanfair and B. A. Korgel, *Cryst. Growth Des.*, 2005, **5**, 1971; (c) S. Xu, S. Kumar and T. Nann, *J. Am. Chem. Soc.*, 2006, **128**, 1054.
- 20 W. E. Buhro, *Polyhedron*, 1994, **13**, 1131.
- 21 (a) T. J. Trentler, S. C. Goel, K. M. Hickman, A. M. Viano, M. Y. Chiang, A. M. Beatty, P. C. Gibbons and W. E. Buhro, *J. Am. Chem. Soc.*, 1997, **119**, 2172; (b) F. D. Wang and W. E. Buhro, *J. Am. Chem. Soc.*, 2007, **129**, 14381.
- 22 T. J. Trentler, K. M. Hickman, S. C. Goel, A. M. Viano, P. C. Gibbons and W. E. Buhro, *Science*, 1995, **270**, 1791.
- 23 (a) X. G. Peng, L. Manna, W. D. Yang, J. Wickham, E. Scher, A. Kadavanich and A. P. Alivisatos, *Nature*, 2000, **404**, 59; (b) S. H. Sun and C. B. Murray, *J. Appl. Phys.*, 1999, **85**, 4325; (c) S. H. Kan, A. Aharoni, T. Mokari and U. Banin, *Faraday Discuss.*, 2004, **125**, 23.
- 24 (a) P. K. Khanna, K. W. Jun, K. B. Hong, J. O. Baeg and G. K. Mehrotra, *Mater. Chem. Phys.*, 2005, **92**, 54; (b) J. H. Chen, M. F. Taib and K. M. Chi, *J. Mater. Chem.*, 2004, **14**, 296; (c) C. Qian, F. Kim, L. Ma, F. Tsui, P. D. Yang and J. Liu, *J. Am. Chem. Soc.*, 2004, **126**, 1195; (d) J. Park, B. Koo, K. Y. Yoon, Y. Hwang, M. Kang, J. G. Park and T. Hyeon, *J. Am. Chem. Soc.*, 2005, **127**, 8433; (e) A. E. Henkes and R. E. Schaak, *Chem. Mater.*, 2007, **19**, 4234.
- 25 (a) Q. Yang, K. B. Tang, Q. R. Li, H. Yin, C. R. Wang and Y. T. Qian, *Nanotechnology*, 2004, **15**, 918; (b) J. L. Wang and Q. Yang, *Dalton Trans.*, 2008, 6060; (c) J. L. Wang and Q. Yang, *Chem. Lett.*, 2008, **37**, 306.
- 26 (a) J. L. Wang, Q. Yang and Z. D. Zhang, *Cryst. Growth Des.*, 2009, **9**, 3036; (b) Y. Sun and Y. Xia, *Science*, 2002, **298**, 2176. In a typical synthesis of In nanoparticles, 0.330 g (1.1 mmol) InCl₃·4H₂O was dissolved in 45 mL of n-propyl alcohol in a Teflon-lined autoclave of a 50 mL capacity, and 0.100 g (1.5 mmol) Zn powder was dispersed into the above solution under agitation. After the solution was stirred for 10 min, the autoclave was sealed, kept at 130 °C for 20 h, and finally cooled to room temperature. The dark-grey products of In nanoparticles were collected, washed with distilled water and absolute ethanol, and then dried under vacuum at 60 °C for further use. In the synthesis of Pd nanoparticles, 0.090 g (0.5 mmol) of PdCl₂ was dissolved in a 40 mL mixture solution of ethanol and polyethylene glycol 400 with a volume ratio of 1 : 1 in an autoclave with a 50 mL capacity under agitation. The autoclave was sealed, kept at 150 °C for 4 h, and finally cooled to room temperature. The dark Pd nanoparticles were obtained after the treatments that are employed in the In nanoparticle synthesis.
- 27 (a) X. Y. Kong, Y. Ding, R. Yang and Z. L. Wang, *Science*, 2004, **303**, 1348; (b) M. Nath and B. A. Parkinson, *J. Am. Chem. Soc.*, 2007, **129**, 11302; (c) G. Z. Shen, Y. Bando, C. Y. Zhi, X. L. Yuan, T. Sekiguchi and D. Golberg, *Appl. Phys. Lett.*, 2006, **88**, 243106; (d) L. Jin, J. B. Wang and W. C. H. Choy, *Cryst. Growth Des.*, 2008, **8**, 3829.
- 28 (a) K. Sano, T. Akiyama, K. Nakamura and T. Ito, *J. Cryst. Growth*, 2007, **301–302**, 862; (b) Q. H. Xiong, J. Wang and P. C. Eklund, *Nano Lett.*, 2006, **6**, 2736; (c) J. L. Wang and Q. Yang, *Cryst. Growth Des.*, 2008, **8**, 660.
- 29 (a) P. E. Fanta, *Chem. Rev.*, 1946, **38**, 139; (b) J. Hassan, M. Sevignon, C. Gozzi, E. Schulz and M. Lemaire, *Chem. Rev.*, 2002, **102**, 1359; (c) A. Klapars, J. C. Antilla, X. H. Huang and S. L. Buchwald, *J. Am. Chem. Soc.*, 2001, **123**, 7727.
- 30 S. Wei, J. Lu, W. C. Yu and Y. T. Qian, *J. Appl. Phys.*, 2004, **95**, 3683.
- 31 E. T. M. Kernohan, R. T. Phillips, B. H. Bairamov, D. A. Ritchie and M. Y. Simmons, *Solid State Commun.*, 1996, **100**, 263.
- 32 M. S. Dresselhaus, G. Dresselhaus, R. Saito and A. Jorio, *Phys. Rep.*, 2005, **409**, 47.
- 33 M. J. Graham, S. Moisa, G. I. Sproule, X. Wu, D. Landheer, A. J. S. Thorpe, P. Barrios, S. Kleber and P. Schmuki, *Corros. Sci.*, 2007, **49**, 31.
- 34 M. H. M. van Weert, O. Wunnicke, A. L. Roest, T. J. Eijkemans, A. Y. Silov, J. E. M. Haverkort, G. W. 't Hooft and E. P. A. M. Bakkers, *Appl. Phys. Lett.*, 2006, **88**, 043109.
- 35 (a) J. Robertson, *Prog. Solid State Chem.*, 1991, **21**, 199; (b) J. Robertson, *Phys. Rev. B*, 1996, **53**, 16302; (c) M. A. Tamor, J. A. Haire, C. H. Wu and K. C. Hass, *Appl. Phys. Lett.*, 1989, **54**, 123.